Synthesis and Characterization of Poly(acrylic acid) Produced by RAFT Polymerization. Application as a Very Efficient Dispersant of CaCO3, Kaolin, and TiO2

ARTICLE *in* MACROMOLECULES · APRIL 2003

Impact Factor: 5.8 · DOI: 10.1021/ma0256744

Synthesis and Characterization of Poly(acrylic acid) Produced by RAFT Polymerization. Application as a Very Efficient Dispersant of $CaCO_3$, Kaolin, and TiO_2

J. Loiseau,[†] N. Doërr,[†] J. M. Suau,[‡] J. B. Egraz,[‡] M. F. Llauro,[§] and C. Ladavière*

UMR 2142-CNRS/bioMérieux Systèmes Macromoléculaires et Immunovirologie Humaine, E.N.S.L., 46, allée d'Italie, 69364 Lyon Cedex 07, France

J. Claverie*

Nanostructured Polymers Research Center, Parsons Hall, 23 College Road, University of New Hampshire, Durham, New Hampshire 03824

Received September 12, 2002; Revised Manuscript Received March 7, 2003

ABSTRACT: Poly(acrylic acid), PAA, was prepared by controlled radical polymerization with reversible addition−fragmentation chain transfer. Using trithiocarbonic acid dibenzyl ester, **1**, and trithiocarbonic acid bis(1-phenylethyl) ester, **2**, as chain transfer agents (CTA), the polymerization is controlled for low ratios [AA]:[CTA]. At higher ratios, the polymerization is plagued by transfer to solvent. Transfer to polymer is also detected at high conversion, as shown by the presence of branches in NMR spectroscopy. In its neutralized form, PAA chains are not all terminated by a thiol end group, as shown by elemental analysis, thiol titration, and MALDI TOF MS. Finally, dispersion of $CaCO_3$, kaolin, and TiO_2 using these PAA reveals that the dispersion characteristics are significantly improved using low-polydispersity PAA.

Introduction

Poly(acrylic acid) (PAA) is widely used as a superabsorbent polymer, a scale inhibitor, and a dispersant.[1] For example, the dispersion of $CaCO_3$ slurries with PAA forms nanoparticles that are subsequently used for paper coating. Around 32 billion lbs of $CaCO_3$ per year is produced for this usage. The mechanism of $CaCO_3$ dispersion relies on the electrostatically driven adsorption of the negatively charged PAA onto the cationic surface of the mineral.[2] As shown below, the average molecular weight and the polydispersity index (PDI = M_w/M_n) strongly influence the quality of the dispersion. By decreasing the PDI, less dispersant is needed, and the viscosity is decreased. For this reason, the preparation of monodisperse PAA on a large scale is of high significance. This grueling task can be accomplished by anionic polymerization of *tert*-butyl acrylate followed by deprotection and purification.[3] However, the preparation of PAAs with less than 0.5% butyl pendant groups is hardly possible. These residual butyl groups have been found to be the source of irreproducibility during mineral dispersion experiments.[4] Using controlled radical polymerization, we can envision the direct preparation of monodisperse PAAs from AA monomer. Nitroxide decomposition in an acidic medium renders nitroxide-mediated polymerizations of AA problematic.[5] Atom transfer radical polymerization (ATRP) is uncontrolled since the polymer can ligate the metal.[6] We have published preliminary data showing how the preparation of PAA with low PDI is possible via reversible addition−fragmentation transfer (RAFT) polymerization, with yields higher than 95%.[7] Other groups have also shown that RAFT is suitable for the preparation of monodisperse polymers in aqueous medium.[8]

This paper offers a detailed report of the polymerization mechanism and kinetics, focusing on chain transfer to polymer and to solvent, and on polymer characterization. First, we show that the polymerization occurs in a controlled fashion until high conversion, generating polymers with low PDI. At the end of the polymerization, chain transfer to solvent becomes important, even in solvents that are not well-known for their capacity to transfer (e.g., dioxane and methanol). Therefore, after neutralization, a large proportion of chains are terminated by a proton and not, as expected, by a thiol. This is confirmed by MALDI TOF mass spectrometry, elemental analysis, and thiol titration. We also demonstrate that chain transfer to polymer occurs for higher molecular weight samples. Not only did we use these well-characterized polymers for the dispersion of $CaCO_3$, but also for kaolin and TiO_2. We show that, due to their low PDI and their controlled architecture, these polymers exhibit excellent dispersant capacity.

Experimental Section

Materials. Acrylic acid, (AA, Aldrich, 99%) was distilled and stored at −40 °C. Ellman's reagent (5,5′-dithiobis(2-nitrobenzoic acid), DTNB, Aldrich, 99%), radical initiator (Init, 4,4′-azobis(4-cyanovaleric acid), 98%, Fluka), radical inhibitor Cupferron (*N*-nitroso-*N*-phenylhydroxylamine ammonium salt, 99%, Aldrich), HPLC internal standards (benzenesulfonic acid hydrate, 97%, Aldrich), and radical inhibitor BHT (2,6-di-*tert*-butyl-4-methylphenol, 99%, Sigma) were used without further purification. The water was ultrapure grade (Purite Analyst 25, ρ = 18.2 MΩ·cm). The ethanol was absolute grade. The other solvents were of analytical grade. $CaCO_3$ (>99%) was a precipitated calcium carbonate, purchased from Solvay (Socal P3, specific surface 13.8 m^2/g). The $CaCO_3$ calcite crystals were scalenohedral (cigarlike shape) with an average size of 250 nm. TiO_2, a rutile type crystal (95%) coated with alumina, was paper grade R-HD2 from Tioxide Corp. (Huntsman). Kaolin

[†] LCPP CPE/CNRS 43, Bd 11 Novembre 1918. BP 2077, 69616 Villeurbanne Cedex. France.
[‡] COATEX, 35 rue Ampère BP8, 69727 Genay Cedex. France.
[§] Service de RMN de la Fédération de recherches des Polyméristes Lyonnais, FR2151/CNRS BP24 69390 Vernaison, France.
* Corresponding authors. E-mail: catherine.ladaviere@ens-lyon.fr; claverie@unh.edu.

10.1021/ma0256744 CCC: $25.00
Published on Web 04/02/2003

Table 1. Polymerization of AA in Refluxing Ethanol[a]

	CTA	[AA]/[CTA]	reaction time (min)	conv (%)	M_n(theo)[b] (g/mol)	M_n(exp) (g/mol)	PDI
1	**1**	50	10	7	125	850	1.3
2	**1**	50	20	40	700	1150	1.4
3	**1**	50	30	66	1200	1450	1.4
4	**1**	50	90	>99	1800	1800	1.4
5	**1**	107	10	31	1200	1000	1.7
6	**1**	107	20	40	1550	1600	1.6
7	**1**	107	30	60	2300	2300	1.5
8	**1**	107	60	85	3300	2650	1.4
9	**1**	107	90	90	3450	2950	1.6
10	**1**	107	120	>96	3700	3000	1.5
11	**1**	98	60	69	2500	2130	1.5
11′	**1**	98	60	69	2500	13300	1.3
12	**1**	98	120	91	3270	2440	1.5
12′	**1**	98	120	91	3270	14300	1.2
13	**1**	98	180	96	3450	2610	1.4
13′	**1**	98	180	96	3450	14900	1.2
14	**2**	100	20	16	600	700	1.5
15	**2**	100	30	45	1600	1300	1.4
16	**2**	100	60	90	3200	2500	1.4
17	**2**	100	90	96	3450	2850	1.4

[a] [CTA]:[Init] = 1:0.1. [AA] = 2.92 mol/L. Entries 11′, 12′, and 13′ respectively correspond to 11, 12, and 13 analyzed with a GPC calibrated with poly(ethylene glycol) standards. All other samples were analyzed with a GPC calibrated with PAA standards. [b] Theoretical $M_n = 0.5 \times$ conversion $\times 94 \times$ [AA]/[CTA]. The factor 0.5 comes from the fact that one CTA generates two PAA chains after neutralization; 94 is the molecular weight of sodium acrylate.

(China clay, >99%), a lamellar pigment from Imerys, had a mean diameter of 0.6 μm, an aspect ratio of 16, and a specific surface of 13.7 m^2/g. Chain transfer agents (CTA) trithiocarbonic acid dibenzyl ester, **1**, and trithiocarbonic acid bis(1-phenylethyl) ester, **2**, were synthesized using procedures detailed in the Supporting Information of ref 7.

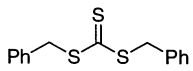

1

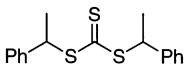

2

RAFT Polymerizations. Results for most polymerizations can be found in the Supporting Information. Typical polymerizations were effected with a monomer concentration of 2.92 mol/L, which corresponds to 25% w:w in ethanol. For dioxane, 25% w:w corresponds to 3.58 mol/L. Polymerization results for both concentrations (2.82 and 3.58 mol/L) are presented in Table 2.

In a 100 mL flask equipped with a cold water condenser, a solution of AA (14.38 g, 0.199 mol) and CTA (**1**, 0.541 g, 0.00186 mol) in ethanol (39.84 g, 0.867 mol) was degassed by gentle nitrogen bubbling. The flask was then brought at 80 °C under nitrogen. The polymerization was started by adding the initiator (4,4′-azobis(4-cyanovaleric acid), 37 mg, 1.32×10^{-4} mol). Aliquots were regularly withdrawn in order to monitor molecular weight and conversion. An excess of an aqueous solution of 10 M NaOH was added to neutralize PAA and unreacted monomer and to cleave the dithio-terminated chains (pH > 9). This mixture was stirred for 2 h and then dried in a vacuum.

Conversion Determination. Each sample was diluted (×1000) in cold water containing Cupferron (0.25% w:w) as radical inhibitor. The conversion was determined by integration of the peak of AA in HPLC (RP Hypersil C18 column, room temperature) using an isocratic water/H_3P0_4 (0.5% v:v)/acetonitrile (10% v:v) eluent (1 mL/min).

Molecular Weight Determination. Molecular weights were determined on a GPC comprising a 515 Waters pump, one or two Ultrahydrogel Linear 7.8 mm × 30 cm columns (mixed bed column with pore size ranging from 120 to 2000 Å) with a guard precolumn, and a 410 Waters refractometer. Elution was performed at 60 °C (0.5 mL/min) using an aqueous buffer ($NaHCO_3$ 0.05 M, $NaNO_3$ 0.1 M, triethanolamine 0.02 M, NaN_3 0.03%). Calibration was relative to PAA standards.[9]

Table 2. Polymerization of AA in Several Solvents Using 1 as CTA ([AA]:[CTA]:[Init] = 500:1:0.1; [AA] = 2.92 mol/L)

	solvent	reaction time (min)	conv (%)	M_n(theo)[b] (g/mol)	M_n(exp) (g/mol)	PDI
1	ethanol	10	16	4 000	3 800	1.8
2	ethanol	20	40	10 000	6 800	2.5
3	ethanol	30	53	12 800	8 500	1.9
4	ethanol	60	78	19 000	10 000	2.0
5	ethanol	90	85	20 500	9 500	2.3
6	ethanol	180	90	22 000	9 450	2.5
7	ethanol	240	94	22 500	8 850	2.7
8	2-propanol	10	7	1 500	2 000	1.8
9	2-propanol	20	54	11 500	4 100	2.3
10	2-propanol	30	67	14 000	4 050	2.4
11	2-propanol	60	84	18 000	4 000	2.6
12	2-propanol	90	91	19 000	4 000	2.6
13	2-propanol	120	94	19 500	3 350	2.9
14	2-propanol	180	96	20 000	2 800	3.4
15	2-propanol	240	100	21 000	3 450	3.1
16	dioxane	20	37	8 700	4 000	2.4
17	dioxane	30	42	9 900	6 000	1.8
18	dioxane	60	62	14 500	9 500	1.7
19	dioxane	90	78	18 500	9 700	1.6
20	dioxane	120	83	19 500	11 000	1.6
21	dioxane	180	88	20 500	11 500	1.7
22	dioxane	240	91	21 400	12 000	1.7
23	dioxane[a]	20	23	5 700	5 400	1.6
24	dioxane[a]	30	39	9 500	10 000	1.3
25	dioxane[a]	60	53	13 000	11 000	1.8
26	dioxane[a]	90	58	14 500	11 000	1.6
27	dioxane[a]	120	61	15 000	11 000	1.9
28	dioxane[a]	180	67	16 500	14 000	1.4
29	dioxane[a]	240	71	17 500	13 000	1.3
30	methanol	10	9	2 300	4 000	3.2
31	methanol	20	19	4 400	2 750	4.6
32	methanol	30	24	5 700	3 000	2.8
33	methanol	60	47	11 000	4 100	1.6
34	methanol	90	61	14 500	5 000	1.6
35	methanol	120	76	18 000	6 200	1.5
36	methanol	180	87	20 000	7 800	1.4

[a] For this set of experiments, [AA]:[**1**]:[Init] = 500:1:0.02 and [AA] = 3.58 mol/L. [b] Theoretical $M_n = 0.5 \times$ conversion $\times 94 \times$ [AA]/[**1**]. The factor 0.5 comes from the fact that one CTA generates two PAA chains after neutralization; 94 is the molecular weight of sodium acrylate.

GPC samples were prepared by inhibiting polymerization with BHT as radical inhibitor, neutralization with sodium hydroxide, and removing solvent in vacuo, and the solid residue was dissolved in the GPC eluent before injection.

Elemental Analysis. One polymer sample was prepared by mixing AA (1.532 g, 0.021 mol), CTA (**1**, 0.212 g, 7.28×10^{-4} mol), ethanol (4.793 g, 0.1 mol), benzenesulfonic acid (0.038 g, 2.43×10^{-4} mol), and radical initiator (0.025 g, 8.9×10^{-5} mol) as described above. The polymerization was stopped at 86% conversion. The reaction medium was separated in two parts. The first part was dried in vacuo, the second one was precipitated with an excess of NaOH (10 N), and the solvent was then removed in vacuo. Elemental analysis results gave overestimations of the %H and %O due to unavoidable hydration of the sample. Therefore, only the ratio of %S and %C, which is not sensitive to hydration, is compared.

Acidic sample: theoretical %S/%C = 0.095; experimental %S/%C = 0.095.

Basic sample: theoretical %S/%C = 0.095; experimental %S/%C = 0.031.

NMR. High-resolution liquid NMR spectroscopy was carried out with a Bruker DRX 400 spectrometer operating at 100.6 MHz for ^{13}C. Spectra were obtained with a 5 mm QNP probe at 333 K. Polymer samples were examined as 30% (w/w) solutions in D_2O. Chemical shift values (δ) were given in reference to the shift of internal Tspd4 (trimethylsilyl-3-propionic acid, 2,2,3,3 sodium salt, $\delta_0 = -2.35$ ppm). Typical accumulations included 70° flip angle, TD = 64 K, and 4.5 s recycle time. Accumulations with gated proton decoupling were about 12 000 scans. Under these conditions, an excellent signal-to-noise was obtained in about 15 h. As for the quantitative aspect, for the protonated carbons of interest (in-chain

CH and terminal CH_2), no difference in relative integrals was observed between acquisitions made under these conditions and those made with much higher delays between pulses (10 s) as well as with both NOE (nuclear Overhauser effect) suppression and delays between pulses, allowing complete relaxation. Chemical shift values and configurational splitting of PAA were influenced by the pH of the solution.

^{1}H NMR: Polymers prepared with **1** (^{1}H, D_2O): 7.4−7.2 (5H, $C_6\mathbf{H}_5$), 2.3−1.9 (27H, C**H**CO_2Na), 1.8−1.3 (54H, C**H**$_2$). Polymers prepared with **2** (^{1}H, D_2O): 7.4−7.2 (5H, $C_6\mathbf{H}_5$), 2.3−1.9 (47H, C**H**CO_2Na), 1.8−1.3 (94H, C**H**$_2$), 1.3−1.2 (3H, C**H**$_3$).

MALDI TOF Mass Spectrometry. The matrix-assisted laser desorption−ionization time-of-flight instrument (Voyager-DE STR, PerSeptive Biosystems, Farmingham, MA) used a nitrogen laser (337 nm) and accelerating voltage of 20 kV. The spectra were the sum of 300 shots. External mass calibration was used (Sequazyme). The poly(acrylic acid) supplied as neutralized sodium salt (20 g/L in water) was prepared in the acid form by ion exchange with a strong acid cation-exchange resin DOWEX (Supelco, Bellefonte, PA). The negative ions were detected with a low mass gate set at 600 in linear mode. The MALDI target was prepared by successive addition of 1 μL of matrix solution (3-β-indoleacrylic acid, IAA, in THF, 0.25 M), 1 μL of the polymer solution, and 1 μL of THF. More details about the preparation of the MALDI TOF targets can be found in the Supporting Information.

Decomposition of the Initiator (Init, 4,4′-azobis(4-cyanovaleric acid)). The procedure was adapted from ref 10. An initiator solution (0.0242 mol/L) in dioxane was prepared, and its absorbance was checked by UV (λ = 250 nm). Using a Peltier heater, the UV cuvette was brought to 80 °C, and the diminution of the absorption A was monitored with time. The rate constant was deduced by plotting ln(A) vs time. By repeating this procedure at several temperatures, an Arrhenius plot was constructed.

Thiol Titration. The sample to analyze was diluted in phosphate buffer (pH = 7.4) containing 0.0012 mol/L of DTNB. Exactly 10 min after mixing, the UV−vis absorption was monitored at 412 nm. Using this methodology, a standard curve was built using benzyl mercaptan, and the response was found to be linear for benzyl mercaptan concentrations ranging from 3×10^{-6} to 4×10^{-5} mol/L. Above this concentration, saturation of the detector was reached. To assess the selectivity of the dosage, it was confirmed that trithiocarbonate **1** did not produce any UV response 10 min after mixing it with Ellman's reagent. For the RAFT PAA sample described in entry 10 of Table 1 (M_n = 3000 g/mol), the theoretical concentration of thiol, calculated on the basis of two thiol end groups per CTA, was 8.6×10^{-5} mol/L. UV−vis measurement indicated no detectable thiol present in the sample. On the basis of the lowest detection limit for benzyl mercapatan (3×10^{-6} mol/L), we concluded that less than 3.4% of the polymer chains contained a thiol end group. For other samples, the maximum amount of SH groups per chain was comprised between 1 and 6%.

Rheological Measurements. The viscosity was measured using a low shear viscosimeter Brookfield (RVT) at 10 and 100 rpm at 20 °C. Only 100 rpm curves are presented in this paper (Figures 10−12), but 10 rpm curves were similar (translated toward high viscosity). In the deflocculation (dispersion) experiment, the mineral solid content was 66% w/w for kaolin, 68% w/w for $CaCO_3$, and 75% w/w for TiO_2. In a typical experiment, a basic solution of PAA in water (25% w:w) was prepared. Then, in a dispersion apparatus comprising a dispersion bowl and a mechanical stirrer (Raynerie type with deflocculation blade), the solution and the mineral were mixed together until the slurry became homogeneous (a few minutes). Viscosity was then recorded, and a new aliquot of PAA was added in order to build the curve viscosity vs dispersant concentration.

Results and Discussion

Chain Transfer Agent (CTA) Selection. Using dithioesters as CTA, Rizzardo was the first to describe the controlled polymerization of AA by RAFT.[11,12] Although the polydispersity index (PDI) was low (1.23), the polymerization was extremely slow (18% yield in 4 h at 60 °C). According to these authors, this strong retardation originates from the intrinsic stability of the intermediate radical in the fragmentation step (Scheme 1) or the slow reinitiation of the fragmented radical or a specific interaction between the radical and the chain transfer agent (CTA).[13]

Scheme 1. Addition−Fragmentation Equilibrium between Propagating Radicals and Dormant Chains in RAFT

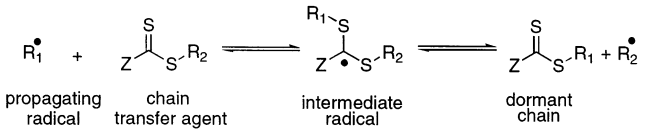

We recently showed that xanthates, first developed by the Rhodia researchers[14] and trithiocarbonates, first described by Rizzardo et al.,[11,15] can be used efficiently for the controlled polymerization of AA into protic medium. This paper describes the AA polymerization mechanism with trithiocarbonates **1** and **2**. The polymerization of AA in ethanol, in the presence of **1** or **2**, is controlled, as shown by the linear evolution of molecular weight vs conversion and medium to low PDIs (Figure 1 and Table 1).

GPC Measurements. Molecular weight and PDI measurement methods were carefully assessed because of their critical nature to the rest of this work. Indeed, GPC of polyelectrolytes is more difficult than GPC of neutral polymers.[16] For low molecular weight samples, it is essential not to separate the polymer from the supernatant by precipitation. For example, for a PAA measured with a PDI = 2.8 (M_n = 7050 g/mol), precipitation/redissolution advantageously translates into a measured PDI = 2.4 (M_n = 8230 g/mol). For very low molecular weight samples that are precipitated, not only M_n increases and PDI decreases systematically but also precipitation of the same sample gives nonreproducible results. During this separation process, many oligomers stay in solution, whereas larger molecular weight chains precipitate. Needless to say, the aqueous GPC[17] had to be calibrated with PAA.[9] The use of aqueous GPC calibrated with PEO standards gave erroneous average molecular weight by a factor as large as 6 and lower PDI (entries 11−13 in Table 1). In addition, GPC measurements agreed well with MALDI TOF mass spectrometry measurements (see below) and NMR end-group determination. For example, for entry 4 of Table 1, M_n = 1800 g/mol by GPC, and the peak with the highest intensity in the MALDI TOF mass spectrometry distribution is m/z = 1700 g/mol. By ^{1}H NMR, phenyl resonances can be used to calculate end groups. For entry 4 of Table 1, M_n calculated by NMR is 2200 g/mol. This slight overestimation of M_n is explained by the presence of transfer to solvent (see below).

The PAA polymer in its acidic form in the dry state could not be kept at room temperature for a prolonged period of time as a sizable fraction of high molecular weight polymers would appear. For example, a polymer was prepared with ratios [AA]:[CTA] and [CTA]:[Init] of respectively 100 and 10 (conversion > 95%). The polymer was kept in its acidic form, but it was solubilized in water at pH = 9 just before GPC analysis. M_w of the polymer, analyzed directly after synthesis, was 5300 g/mol (PDI = 1.6), and it changed to 6800 g/mol

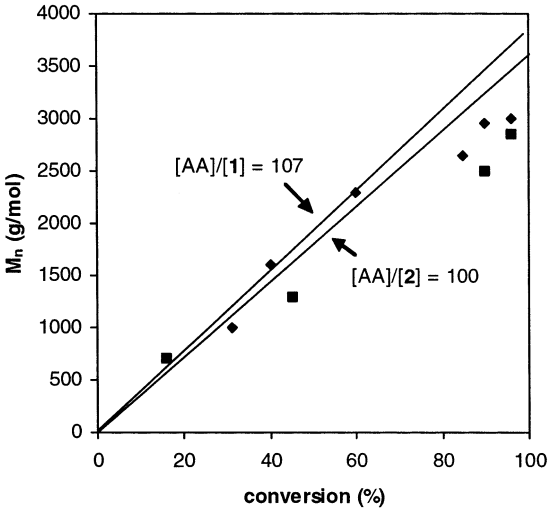

Figure 1. M_n vs conversion for chain transfer agent **1** (■) and **2** (◆). Line: theoretical M_n (= 0.5 × conversion × 94 × [AA]/[CTA]). The factor 0.5 comes from the fact that one CTA generates two PAA chains after neutralization. 94 is the molecular weight of sodium acrylate.

Scheme 2. Neutralization of PAA with NaOH and Hydrolysis of Trithiocarbonate Moiety

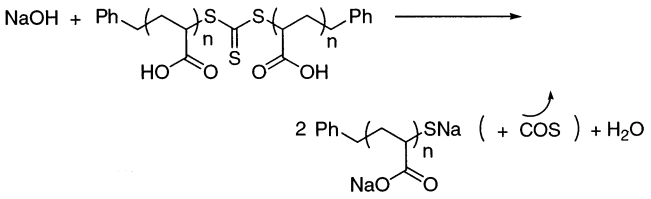

(PDI = 1.9) after 28 days at 4 °C. In contrast, PAA−Na (the polymer fully neutralized by NaOH) can be kept in the dry state for months. We hypothesize that in the bulk very small amounts of trithiocarbonates might decompose through a radical pathway,[18] leading to a slow and irreversible radical cross-linking of the polymer. When the polymer is neutralized with NaOH, the trithiocarbonate should be hydrolyzed to thiol (Scheme 2).[19] Alternatively, a reviewer has proposed that the increase in molecular weight may be due to strongly interacting dimer bridges formed during acid storage.

Influence of [AA]/[CTA] and Influence of the Solvent. When [AA]/[CTA = **1**] = 50, the polymer molecular weight is above the theoretical molecular weight (entries 1−3, Table 1) because the first transfer between **1** and a propagating radical is less efficient than the subsequent transfer between a dormant chain and a propagating radical.[20] M_n follows the evolution predicted for a degenerative transfer process with a low chain transfer constant: it is higher than theoretical molecular weight at first, and it eventually catches up with the linear profile.[7,21] As expected, the phenethyl radical is a better leaving group than the benzyl one, shown by a better agreement between theoretical and experimental molecular weight for CTA **2**.[7,21]

For both CTAs in ethanol, 2-propanol, and dioxane, when [AA]/[CTA] ≥ 100, the PAA molecular weight corresponds to theoretical molecular weight as long as conversion is less than 30% (Figures 1−3). The aforementioned effect of a slow initial chain transfer is masked because the chains are longer. In methanol (Figure 4), this effect is still visible because the polymerization temperature is lower than for other solvents, resulting in lower chain transfer constants.

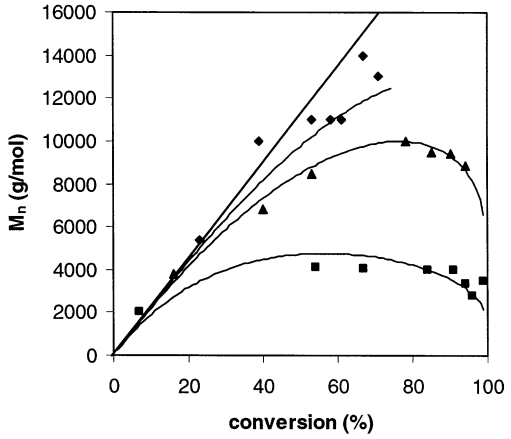

Figure 2. M_n vs conversion for different solvents. [AA]:[**1**]:[Init] = 500:1:0.1 in 2-propanol (■), ethanol (▲), and dioxane (◆). In dioxane, polymerization reaches 80% in 2 h. The straight line corresponds to theoretical molecular weight for a controlled polymerization (see caption Figure 1); curved lines correspond to the molecular weight obtained with eq 4 (controlled polymerization with chain transfer to solvent).

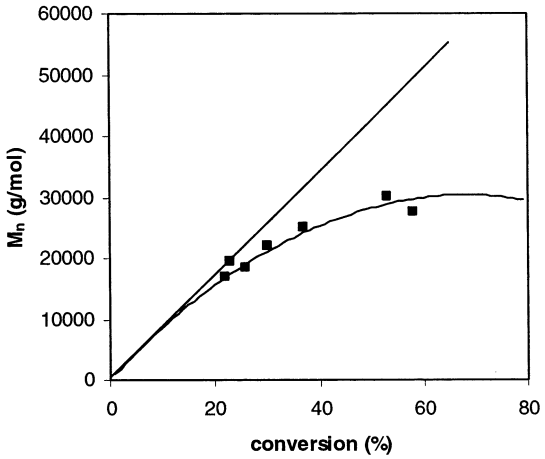

Figure 3. M_n vs conversion in dioxane. [AA]:[**1**]:[Init] = 2000:1:0.16. The straight line corresponds to theoretical molecular weight for a controlled polymerization (see caption Figure 1); curved lines correspond to the molecular weight obtained with eq 4 (controlled polymerization with chain transfer to solvent).

For all solvents, when [AA]/[CTA] ≥ 100, the polymer molecular weight is lower than the expected molecular weight for conversion greater than 50%. This discrepancy increases with increasing conversions and increasing [AA]:[CTA] (Figures 2−4 and Table 2). The presence of a nondegradative transfer process (a transfer reaction where the transferred radical can reinitiate) can account for this phenomenon. Transfer to monomer can be ruled out, as increasing the monomer concentration from 2.92 to 3.58 mol/L results in less transfer (Table 2, entries 16−22 vs 23−29). A similar argument can be used to discard chain transfer to the polymer end groups (benzyl and phenethyl) or to the initiator (CH_2 in α of COOH), as one would expect to see lower transfer for increasing ratios [AA]:[CTA] ratios and [AA]:[Init] ([AA] constant, see comparison of Tables 1 and 2). Therefore, we ascribe this phenomenon as transfer to solvent. The contribution of transfer to solvent could have been attenuated by polymerizing at higher monomer concentration such as 50 wt % in solvent, but at such high concentrations, viscosity increase results in a loss of control and broad PDIs.

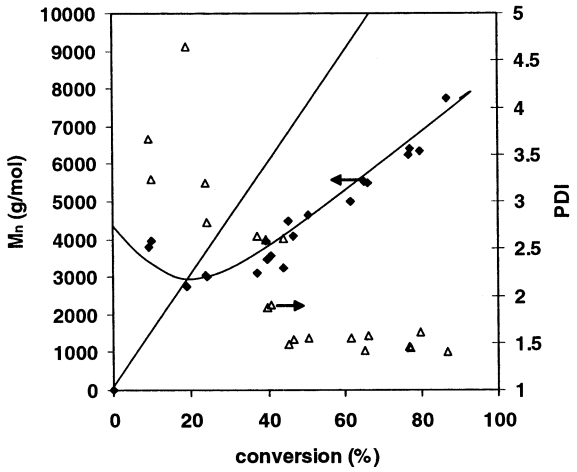

Figure 4. M_n (◆) and PDI (△) vs conversion in methanol (T = 67 °C) when [AA]:[**1**]:[Init] = 500:1:0.1. The straight line corresponds to theoretical molecular weight (see caption Figure 1); the curved line is to guide the eyes.

The transfer constant to 2-propanol, C_{tr}(2-propanol), in AA polymerization was measured by Pichot ($C_{tr} = 2 \times 10^{-3}$).[22] Except for the case of 2-propanol, which has a "high" transfer constant, we were surprised at first at the marked influence of transfer to solvent in RAFT polymerizations. In conventional AA polymerization, transfer to solvent is "masked", as the final product is usually a cross-linked gel. A closer scrutiny indicates that a moderate value of transfer constant to solvent will have consequent repercussions during a RAFT polymerization conducted to high conversion. Indeed, the concentration of polymer chains created by transfer to solvent (rate k_{tr}), [D], is given by eq 1.

$$\frac{d[D]}{dt} = k_{tr}[S][P^*] \quad (1)$$

[S] is the solvent concentration, and [P*] is the radical concentration. The propagation rate is

$$\frac{d[M]}{dt} = -k_p[M][P^*] \quad (2)$$

where [M] is the monomer concentration. The ratio of eqs 1 and 2 yields after integration eq 3:

$$[D] = -C_{tr}[S] \ln \frac{[M]}{[M]_0} \quad (3)$$

Ignoring the contribution of chains created by radical initiator decomposition ([CTA]:[Init] = 10:1) and assuming that transfer to CTA is relatively fast, the total number of chains in the polymerization is CTA + [D]. At low conversion, where CTA is not consumed, this expression overestimates the total number of chains. Therefore, the number-average degree of polymerization vs conversion, p, is given by eq 4.

$$X_n = \frac{[M]_0 p}{[CTA] - C_{tr}[S] \ln(1 - p)} \quad (4)$$

Using experimental values of M_n and conversion p (Table 2), the chain transfer constant to 2-propanol ($C_{tr} = 2.4 \times 10^{-3}$), ethanol ($C_{tr} = 4.7 \times 10^{-4}$), and dioxane ($C_{tr} = 3.9 \times 10^{-4}$) can be evaluated by a nonlinear optimization. Figures 2 and 3 compare experimental M_n vs conversion and M_n calculated using eq 4 (curved plain lines), which agree well. To use eq 4 for the trithiocarbonates **1** and **2**, one has to replace [CTA] by 2 [CTA] as two dormant chains are obtained per CTA. Although they have nearly the same C_{tr}, deviation from linearity is less pronounced in dioxane than ethanol, because the solvent concentration is higher for ethanol ([ethanol] = 13.71 mol/L) than for dioxane ([dioxane] = 8.81 mol/L). Deviation to linearity, indicative of transfer, is easily observed in the case of dioxane at ratio [AA]:[CTA] = 2000 (Figure 3). In methanol polymerization (Figure 4), M_n increased linearly with conversion but was always below the theoretical M_n, indicating that transfer to solvent occurs.

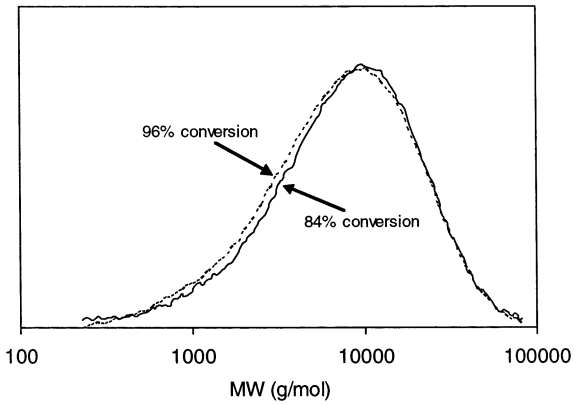

Figure 5. Molecular weight distribution of samples collected at 84% (solid line) and 96% (dotted line) conversion for [AA]:[**1**]:[initiator] = 500:1:0.1 in 2-propanol.

For low ratio [AA]:[**1**], transfer to solvent becomes only apparent at high conversion when the propagation rate is significantly decreased, but the rate of transfer which does not depend on monomer concentration is nearly unchanged. This is easily observed by comparing the GPC molecular weight distribution of a sample obtained at 84% conversion and a sample of the same polymerization at 96% conversion (Figure 5). Instead of the expected displacement of the molecular weight distribution toward higher molecular weights, a large number of very short oligomers appear. The molecular weight at the peak of the distribution (M_p) follows the expected linear relationship with conversion, as the peaked part of the distribution contains a large number of untransferred dormant chains that are readily reactivated through the RAFT mechanism. Thus, when the polymer is precipitated before GPC analysis, all of the transferred chains (very low molecular weight) disappear, and theoretical and experimental molecular weights better agree. Using GPC with light scattering and viscosimetric detection, the low molecular weight tail of the distribution was underestimated because of the intrinsic poor sensitivity of the detector for very low molecular weight fractions and the variation of dn/dc with molecular weight in this region (due to end groups). Further work in this area is in progress.

To conclude this section on transfer to solvent, it appears that the RAFT process readily controls the polymerization when the [AA] is large enough. At low monomer concentration (high conversion), transfer to solvent becomes important, resulting in the termination of long chains and the generation of new short dormant chains. Fortunately, for low [AA]/[CTA], transfer occurs only very late in the polymerization (Figure 6). Therefore, it is possible to polymerize in a "controlled" fashion

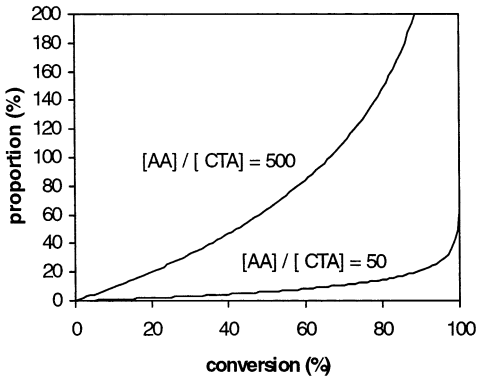

Figure 6. Proportion of chains transferred to ethanol vs conversion for [AA]/[CTA] = 50 and [AA]/[CTA] = 500, as calculated from eq 3 ([AA] = 2.92 mol/L, [ethanol] = 13.71 mol/L, one dormant chain per chain transfer agent). At 50% conversion, only 6% of the chains have undergone a transfer to ethanol when [AA]/[CTA] = 50, whereas 63% of the chains are transferred when [AA]/[CTA] = 500.

Table 3. Polymerization of AA in Dioxane Using 1 as CTA ([AA]:[1]:[Init] = 2000:1:0.16; [AA] = 2.92 mol/L)

	reaction time (min)	conv (%)	M_n(theo)[a] (g/mol)	M_n(exp) (g/mol)	PDI
1	10	7	7100		
2	20	22	20 500	17 000	2.3
3	30	23	22 000	19 500	2.5
4	60	26	24 500	18 500	2.3
5	90	30	29 000	22 000	2.5
6	120	37	35 000	25 000	2.3
7	180	53	50 500	30 000	2.5
8	280	58	55 500	27 500	2.6

[a] Theoretical $M_n = 0.5 \times$ conversion $\times$ 94 $\times$ [AA]/[**1**]. The factor 0.5 comes from the fact that one CTA generates two PAA chains after neutralization; 94 is the molecular weight of sodium acrylate.

up to high conversion. For higher [AA]/[CTA], transfer becomes noticeable even at low conversion.However, we do not discard the presence of other less important transfer reactions (transfer to monomer, end groups, and initiator). As **1** and **2** are not water-soluble, specific water-soluble chain transfer agents are at this time prepared and tested in water in which transfer to solvent is expected to be low.

Transfer to Polymer. Because of the presence of a tertiary hydrogen α to the carbonyl group, acrylic polymers tend to be branched through transfer to polymer.[23] In nitroxide-mediated polymerization, transfer to polymer has been detected by NMR, but quantification of intramolecular vs intermolecular transfer is based on MALDI TOF spectrometry.[24] To quantify transfer to polymer in PAA, all carbons were identified by ^{13}C NMR. A typical spectrum is shown in Figure 7.

Neither the quaternary carbon of the grafting site (at 48.5−50 ppm, see Table 4) nor the carbonyl of the branch point is suitable for quantification due to their very weak resonance and their low concentration (one carbon per grafting site), absence of NOE, and long relaxation time for the last one. Both methyne and methylene carbons were easier to detect (three or two carbons by branching point and full NOE). We expected the CH_2 in α of the grafting site to be deshielded (about 3.7 ppm on the basis of a chemical shift substituent increment scheme for alkanes[25]), and it was observed at 38−39 ppm. However, the resolution was not good enough for a reliable quantification.

As for the methyne carbon in β position, two different situations may occur as shown in Scheme 3.

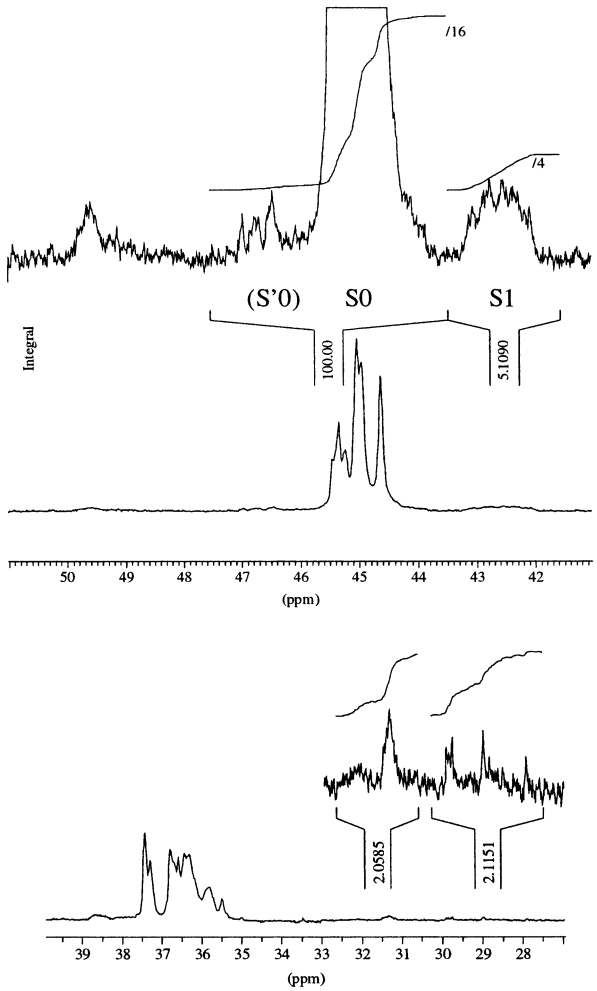

Figure 7. ^{13}C NMR (100.6 MHz) spectra of PAA (neutralized) in D_2O at 60 °C: top, enlargement of the low-field resonance region (methyne and quaternary carbon); bottom, enlargement of the high-field resonance region (methylene carbons).

The intermolecular transfer generating a long branch (LB) should give rise to three new CH resonances (S_1) expected at lower field (about 2.2 ppm) compared to the main-chain CH (S_0). An intramolecular transfer should give rise to only two new CH (S_1), whereas the third one situated on the short branch itself (SB) should overlap the main CH resonances (tentative assignment: S'_0). We used the methyne carbons for quantification due to the good resolution of S_0 and S_1 resonances (Figure 7, Table 4).

Estimation of the grafting at the transfer site, expressed in moles per 100 inserted monomer units (LB), on the basis of exclusive intermolecular transfer and calculated from the methine (CH) carbon integrals is given by the following expression

$$\mathrm{LB} \cong 100\,\frac{{}^1/_3 S_1}{S_0 + {}^4/_3 S_1} \qquad (5)$$

where S_1 is the integral of the three CH carbons α to the branch Cq (if both transfers are present S_1 = 3LB + 2SB) and S_0 is the integral of all other CH carbons. In this expression, among terminal repeat units of both main-chain and branches, those which do not have methine carbons (CH_2-CH_2-COOH end groups) have been neglected. This approximation holds because higher molecular weight polymers were analyzed (M_n = 16 000

Scheme 3. Representation of Branches Obtained by Transfer to Polymer and Specific Resonance Areas Chosen for Quantification

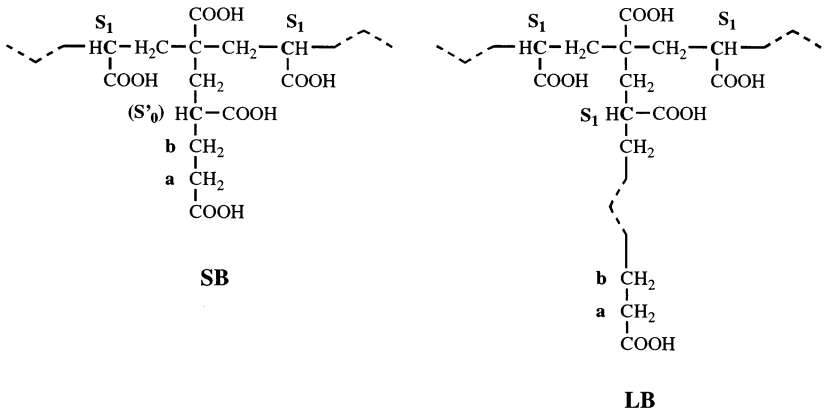

Table 4. Assignments of the ^{13}C NMR Spectrum of the PAA in D_2O at 60 °C (See Figure 7)

peak[a]	δ (ppm)[b]	assignment
B	27.5−30	end group $-\boldsymbol{C}H_2-CH_2-COOH$
A	30.5−33	end group $-CH_2-\boldsymbol{C}H_2-COOH$
	35−38	main chain $-\boldsymbol{C}H_2-$
	38−39	$-\boldsymbol{C}H_2-$ adjacent to branch
S_1	41.8−43.4	$-\boldsymbol{C}H$ adjacent to branch
S_0	43.65−48	main-chain $-\boldsymbol{C}H$
(S'_0	46−48	−CH SB part of S_0)
	48.5−50	(SB + LB) branch quaternary $\boldsymbol{C}$

[a] See Scheme 3 for peak labels. [b] Chemical shift values are slightly dependent on the neutralization ratio (pH).

g/mol). Estimation of branching, as given in eq 5, includes only carbons of the same nature and does not require spectra obtained with NOE suppression and complete relaxation (see experimental part).

For this study on branching, two different samples were prepared. For the first sample, the polymerization was stopped at 79% conversion; no branch was detected for this sample. For the other one, the reaction was polymerized for 3 h, and a significant amount of branches was detected (1.6% based on exclusive intermolecular LB). It is also possible to quantify the total transfer (inter + intra) from integral values of a and b (Scheme 3). Nevertheless, this calculation requires the relaxation of terminal carbons a and b to be fast (see experimental part) and the main-chain end groups not to be counted under the integrals of a and b. In our sample, the integral values of carbons a and b are equal to 2.1 = LB + SB, but $S_1 = 5.1 = 3LB + 2SB$, giving SB = 1.2 and LB = 0.9. Thus, *under the above assumptions*, an estimation of total transfer is 1.9% (2.1/108.9 = 1.9%, 55% intramolecular and 45% intermolecular). Nevertheless, a deviation of only 10% in the value of the a and b integrals translate into a very large deviation (>20%) into the relative amount of intra- and intermolecular transfer (SB/SB + LB). In contrast, the total amount of transfer is little affected by the value of a and b.

According to NMR spectroscopy, linear polymers are obtained early in the polymerization, whereas 1.9% branches are generated in the later stage of the polymerization. Some of these branches are intramolecular (putative value 1.1%). Thus, transfer to polymer occurs *in the later stage of the polymerization* when the concentration of polymer is high enough, and the propagation rate is decreased. These findings differ from those of Lovell,[23,26] who has elegantly shown that for dilute solution radical polymerizations (typically $[M_0]$ < 10% w:w) branching level increases steadily with

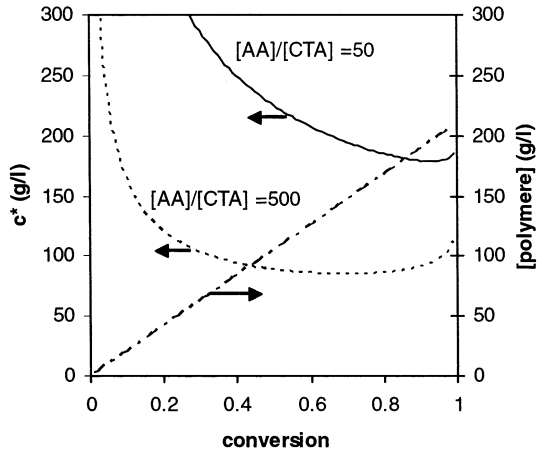

Figure 8. Plot of the critical overlapping concentration c^* calculated using eq 6 (left axis) and of the polymer concentration (right axis) against conversion in a RAFT polymerization of AA (solid line, [AA]/[CTA] = 50; dashed line, [AA]/[CTA] = 500 calculated using $[M]_0 = 2.92$ M). In eq 6, M_n has been calculated using eq 4. When [AA]/[CTA] = 500 (50), the system crossovers from dilute regime to concentrate regime at 42% (86%) conversion.

decreasing initial monomer concentration because the local [P]/[M] ratio increases in the vicinity of the growing radical. (The polymer concentration stays constant whereas the monomer concentration decreases.) Thus, for a dilute polymerization, most transfers are intramolecular. Above the critical overlapping concentration, c^*, intermolecular chain transfer dominates the polymerization due to polymer chain entanglement. Therefore, for concentrated polymerizations (typically $[M_0]$ > 20% w:w > c^*) most of the polymerization (except at very low conversion) occurs in this concentrated regime where polymer chains overlap and the branching level is independent of the initial monomer concentration. The main difference between conventional radical polymerization, as described by Lovell, and controlled radical polymerization is that c^* will vary by 1 order of magnitude during the controlled polymerization. In Lovell's study, c^* varies by no more than 15%. Using Lovell's notations, c^* is given by

$$c^* = \frac{1.3}{N_a M_n^{0.5}} \left(\frac{M_0}{\alpha^2 l^2 C_\infty} \right)^{1.5} \qquad (6)$$

where M_0 is the repeat unit molar mass, N_a the Avogadro constant, α is the expansion parameter which

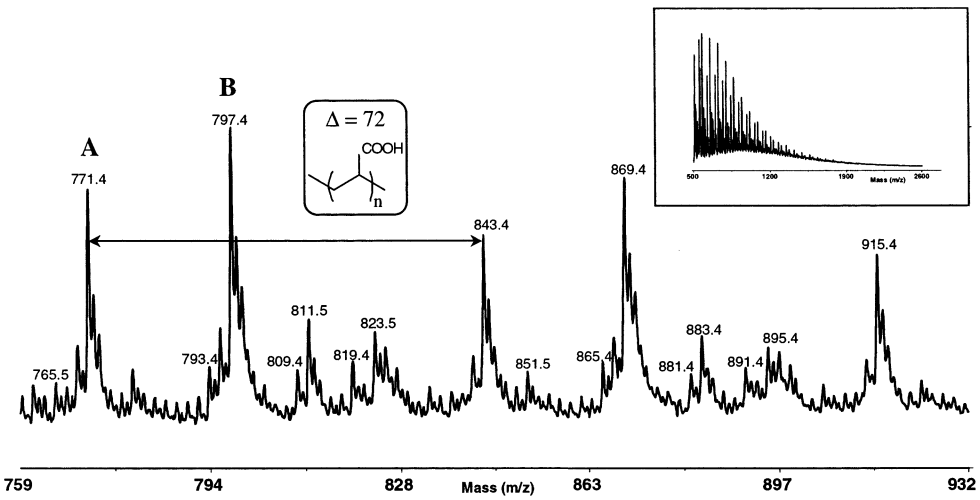

Peak	Product
A	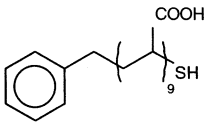
B	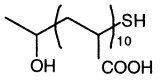

Figure 9. Negative ion MALDI TOF mass spectrum of poly(AA) ($M_{n(GPC)}$ = 730 g/mol, PDI = 1.46, conversion 12%) obtained in linear mode (IAA matrix). Minor peaks (see Supporting Information) may be attributed to $CH_3CH(OH)-(AA)_{10}-H$ (m/z = 765.5), $PhCH_2-(AA)_4-S(C{=}S)S-(AA)_3-CH_2Ph$ (m/z = 793.4), $PhCH_2(AA)_9CH{=}CHCOOH$ (m/z = 809.4), and $PhCH_2(AA)_{10}H$ (m/z = 811.5).

relates the characteristic size of the pelote compared to the size of an ideal pelote ($\alpha \approx 1.2$), C_∞ is the characteristic ratio ($C_\infty \approx 8$)[26] and l is the mean distance of a C−C in the backbone (l = 154 pm).[27] In a controlled polymerization, where M_n increases with conversion, c^* will markedly decrease as the polymerization progresses. In Figure 8, c^* values are plotted against conversion, for a polymerization where [AA]:[CTA] is 50 and 500. Figure 8 shows that, for a significant part of the polymerization reaction, the polymer concentration is below c^*, and we would expect, on the basis of Lovell's findings, to observe a significant amount of intramolecular branching, whereas we only observe branching (intra and inter) in the latest stage of the polymerization. Although we have not clarified this issue further, the rate of transfer to polymer may not be impeded by the "diffusional" motion of the macromolecules because we work with low molecular weight samples. Instead, polymer and monomer can be considered as uniformly distributed in the solvent, and only "chemical" factors dictate the occurrence of transfer. Thus, under this hypothesis, the classical Flory prediction[28] that transfer frequency increases sharply at high conversion could be verified. Further work, including determination of intrinsic viscosities and light scattering determination of branching ratios, is in progress.

Detection of Polymer End Groups. After polymerization and neutralization of PAA with NaOH, most chains should be cleaved from the trithiocarbonate by nucleophilic attack of OH^- onto the thiocarbonyl function (Scheme 2).[19] Large amounts of NaOH are necessary to neutralize PAA in an exothermic reaction (pH at the end of the reaction is above 8). Measured molecular weights are always equal to or less than the theoretical one (and not equal to double the theoretical one), indicative of cleavage.

MALDI TOF mass spectrometry (MS) was used to detect the PAA end groups. Polymers with molecular weights ranging from 700 to 4000 g/mol were analyzed. The negative MALDI TOF mass spectra of neutralized PAA obtained in the linear mode with an acceleration of 20 kV are depicted in Figures 9 and 10. We have not been able to obtain a spectrogram of a polymer in its "trithiocarbonate" form (directly from the reaction pot). MALDI TOF mass spectra of half-neutralized PAA (see Supporting Information) were similar to fully neutralized samples (Figures 9 and 10). Others have argued that MALDI TOF analysis of polymers terminated by dithiocarbamates is problematic due to the putative fragmentation of the end group during desorption.[29]

A good agreement is observed between the molecular weight of the MALDI TOF MS highest peak and that of the GPC peak (see captions of Figures 9 and 10). In low molecular weight PAA samples prepared in ethanol (Figure 9), the predominant presence of ethoxy initiated chains is an unambiguous proof of transfer to solvent. Because of transfer to solvent, H-terminated chains are also observed in high proportions in high molecular weight samples (Figures 9 and 10). In our first report (see Figure 2 in ref 7), proton-terminated chains were the major species detected by MALDI TOF mass spectrometry. These polymers were obtained at very high conversion (>95%) when most chains have undergone transfer to solvent.

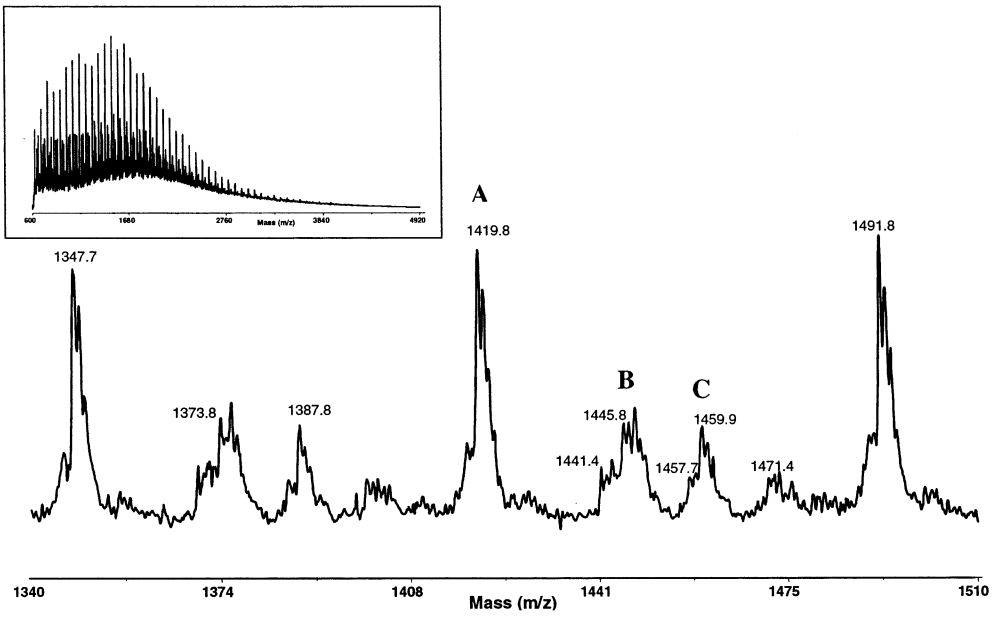

Peak	Product
A	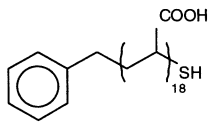
B	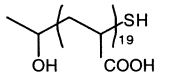
C	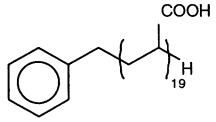

Figure 10. Negative ion MALDI TOF mass spectrum of poly(AA) ($M_{n(GPC)}$ = 1590 g/mol, PDI = 1.58, conversion 83%) obtained in linear mode (IAA matrix). Minor peaks (see Supporting Information) may be attributed to $PhCH_2-(AA)_8-S(C=S)S-(AA)_8-CH_2Ph$ (m/z = 1441.4) and $PhCH_2(AA)_{18}CH=CHCOOH$ (m/z = 1457.7).

Because MALDI TOF MS is not quantitative, the thiol concentration was assessed using Ellmann's reagent (see experimental part). Surprisingly, no thiol was detected in the polymer during the polymerization or after neutralization. During the polymerization, the absence of thiol end groups indicates that the putative solvolysis of the trithiocarbonate (eq 7) is not occurring. After neutralization, the expected thiol may be oxidized in a disulfide.

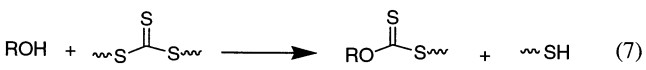

(7)

Our elemental analysis findings were even more surprising. The acidic form of the polymer contained exactly the theoretical amount of sulfur. After neutralization with an excess of NaOH, the polymer lost considerable amount of sulfur (more than 70%). A basic decomposition of thiol into volatile products may explain this phenomenon, but we could not write a satisfactory mechanism to account for it.

Polymerization Kinetics. RAFT polymerization is subject to retardation effects that have been attributed to the intrinsic stability of the intermediate radical during the addition fragmentation step.[13,30,31] Because of their stability and subsequent increased lifetime, these intermediate radicals have been detected by ESR. Recent studies by Monteiro et al. have suggested that retardation occurs through the termination of a propagating polymer chain with the intermediate radical.[32]

RAFT of AA occurs with considerable retardation relative to conventional AA polymerization under similar conditions. Before embarking upon a more detailed discussion of the polymerization kinetics, we checked that initiator decomposition lifetime is long enough to ensure a sufficient radical flux during the polymerization. Indeed, as measured by the disappearance of the 350 nm chromophor by UV spectroscopy (see experimental part), the rate of decomposition of the initiator (4,4′-azobis(4-cyanovaleric acid)) in ethanol is expressed by $k_d = 5.26 \times 10^{12} \exp(-13500/T)\ s^{-1}$. At 80 °C, the half-life of initiator is therefore 2 h. Initiator decomposition is not accelerated by the presence of the trithiocarbonate, as shown by following the rate of disappearance of CTA **1** (by UV, λ = 433 nm) in an equimolar mixture of **1** and initiator. (The initiator absorbance is

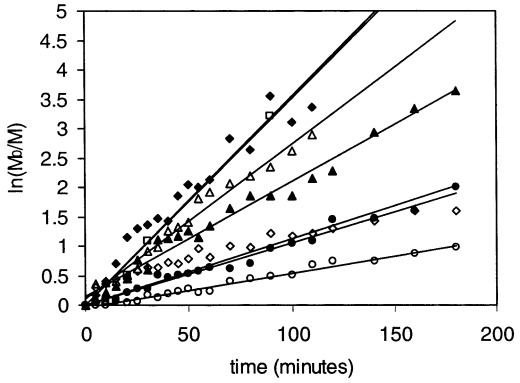

Figure 11. Ln(M_0/M) vs time for several polymerization conditions: (◆) polymerization in ethanol with [AA]/[**1**] = 492, [Init]/[**1**] = 1.0, [AA] = 2.92 mol/L, T = 80 °C; (□) polymerization in ethanol with [AA]/[**1**] = 50, [Init]/[**1**] = 0.1, [AA] = 2.92 mol/L, T = 80 °C; (△) polymerization in ethanol with [AA]/[**1**] = 107, [Init]/[**1**] = 0.07, [AA] = 2.92 mol/L, T = 80 °C; (▲) polymerization in ethanol with [AA]/[**1**] = 500, [Init]/[**1**] = 0.12, [AA] = 2.92 mol/L, T = 80 °C; (◇) polymerization in dioxane with [AA]/[**1**] = 500, [Init]/[**1**] = 0.12, [AA] = 2.92 mol/L, T = 80 °C; (●) polymerization in methanol with [AA]/[**1**] = 500, [Init]/[**1**] = 0.10, [AA] = 2.92 mol/L, T = 67 °C; (○) polymerization in 2-propanol with [AA]/[**1**] = 107, [Init]/[**1**] = 0.13, [AA] = 2.92 mol/L, T = 77 °C.

entirely masked by the trithiocarbonate one.) The rate of disappearance of **1** was equal to the initiator decomposition rate (in the absence of **1**), indicating that, as expected, initiator decomposition is not affected by the presence of **1**. Thus, the radical flux generated through initiator decomposition is high enough for polymerizations lasting a few hours.

The polymerization kinetics are first-order in monomer concentration, as shown in Figure 11. Because of the fast polymerization, the data are scattered at short time. When [AA] = 2.92 mol/L, [AA]:[**1**] = 500:1, and [**1**]:[init] = 1:0.1, a remarkable solvent effect can be observed. From slow to fast, solvents can be rated in the following order: 2-propanol < dioxane < ethanol. Methanol is not part of this scheme, as we ran methanol polymerizations at 67 °C instead of 80 °C. As expected for a protic solvent, ethanol polymerization is faster than dioxane. The position of 2-propanol is more difficult to explain.

Because the polymerizations have apparent first-order kinetics, we can rule out a Tromsdorff effect which occurs under the same conditions for a noncontrolled polymerization. Surprisingly, ethanol polymerizations having the same initiator concentration but different CTA concentrations (diamonds and open squares in Figure 10) have similar reaction rates. This contrasts with the findings of Goto et al.,[30] who found that for styrene polymerization the CTA concentration markedly influences the polymerization rate. We are investigating this issue further, using on-line sensors (such as Raman spectroscopy) and calorimetric reactors, to diminish the scattering of our data.

Dispersion of Mineral. We used the RAFT made PAA to disperse minerals, especially $CaCO_3$. At neutral pH, $CaCO_3$ solubility is low ($<10^{-4}$ mol/L), and this compound is almost entirely crystallized in water.[33] Surface ions constituting the surface of these crystals are either Ca^+ or CO_3^- [34] with an excess of Ca^+, thus conferring a positive charge to the surface on which PAA adsorbs.[35] The adsorption mechanism of PAA onto $CaCO_3$ surface first involves the adsorption of the shortest PAA chains, as these can diffuse first to the surface.[36] These chains are then displaced by medium length PAA chains through an entropically favorable process. At this stage, surface Ca^+ are complexed, and the crystal is protected by a globally negative PAA hairy layer. Longer PAA chains no longer approach the surface because of the very large electrostatic repulsion between the globally negative free polymer coil and the negatively charged crystal surface. Therefore, in polydisperse PAA samples, only chains with a precise molecular weight (around 3000 g/mol) are adsorbed: shorter and longer chains stay in solution.[36] For applicative purposes, it is desirable to use the lowest amount of dispersant and to obtain a slurry with the lowest viscosity. Since both short and long chains do not contribute to colloidal stabilization and since chains in solution (especially the long ones) increase the viscosity, it is necessary to prepare PAA with a molecular weight of around 3000 g/mol[35] and the lowest possible polydispersity index (PDI = M_w/M_n). The adsorption mechanism of PAA onto kaolin or Al_2O_3 has been described in the literature to be in essence related to the one of PAA onto $CaCO_3$.[37] The TiO_2 we used for this experiment is coated with 5% alumina. To our knowledge, we present here the first report of mineral dispersion using "monodisperse" PAA.

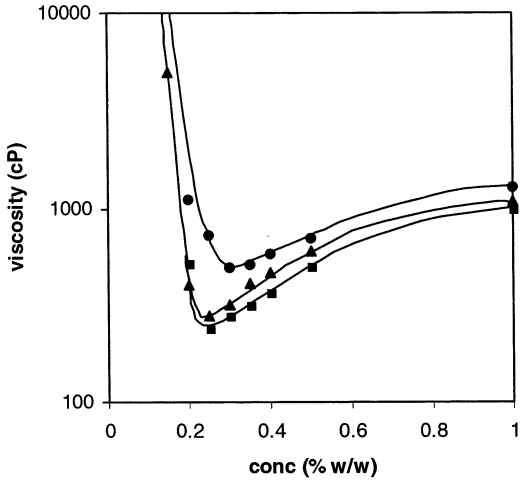

Figure 12. TiO_2 dispersion using PAA dispersant: viscosity (at 100 rpm) vs concentration of dispersant measured as the weight percentage of dry dispersant relative to the weight of dry TiO_2: (◆) commercial PAA (M_n = 2800 g/mol, PDI = 3); (▲) PAA obtained by fractionation process (M_n = 3100 g/mol, PDI = 2); (■) PAA obtained by RAFT using **1** (M_n = 3100 g/mol, PDI = 1.6).

In a typical dispersion experiment, a slurry of mineral in water (typically 66% in weight) was mixed with a certain amount x of PAA (Figures 12−14). Brookfield viscosity (measured at 100 rpms) vs x shows a typical bell curve; when not enough dispersant is present, the viscosity is high due to the presence of partially flocculated particles. The viscosity decreases with x, until a minimum is reached, after which the viscosity increases as a result of the presence of nonadsorbed water-soluble polymer in solution. When comparing the performance of RAFT polymer vs a PAA made by a conventional radical process, the saturation amount at which minimum viscosity is reached is lowered (TiO_2 dispersion, Figure 12). This is due to the narrower molecular weight distribution; in RAFT, most chains have the right molecular weight to contribute to the adsorption process. In conjunction with the reduction

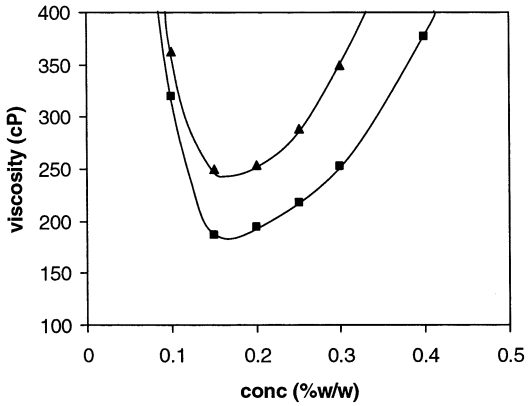

Figure 13. Kaolin dispersion using PAA dispersant: viscosity (at 100 rpm) vs concentration of dispersant measured as the weight percentage of dry dispersant relative to the weight of dry kaolin. (▲) Commercial PAA (M_n = 2800 g/mol, PDI = 3), (■) PAA obtained by RAFT using **1** (M_n = 3100 g/mol, PDI = 1.6).

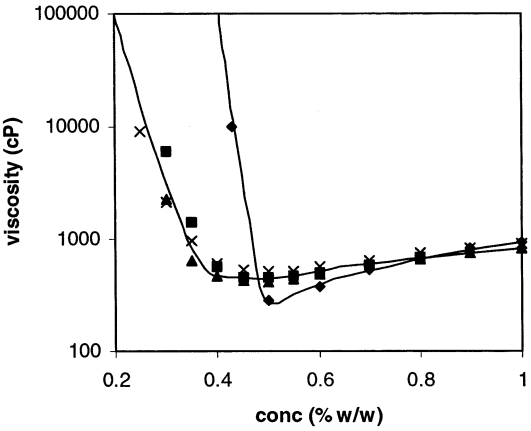

Figure 14. $CaCO_3$ dispersion using PAA dispersant: viscosity (at 100 rpm) vs concentration of dispersant measured as the weight percentage of dry dispersant relative to the weight of dry $CaCO_3$: (◆) commercial product (M_n = 2800 g/mol, PDI = 3); (×) PAA made by RAFT with **2** (M_n = 3200 g/mol, PDI = 1.5); (■) PAA made by RAFT with **1** (M_n = 4000 g/mol, PDI = 1.6); (▲) PAA made by RAFT with **1** (M_n = 4800 g/mol, PDI = 1.7).

of the saturation amount, the viscosity decreases with decreasing PDI as fewer chains are in the aqueous phase. If the adsorption mechanism seems to be experimentally confirmed for TiO_2 dispersion, kaolin (Figure 13) and $CaCO_3$ (Figure 14) dispersions are more complicated. In the kaolin dispersion, the viscosity is reduced by using a less disperse polymer, but the saturation amount is unchanged. In the $CaCO_3$ dispersion, the saturation amount is drastically reduced, but the viscosity is actually slightly higher for more monodisperse polymers. To our surprise, the rheological profile is barely changed when the average molecular weight varies from 3200 to 4800 g/mol, seemingly indicating that the viscosity is more affected by the PDI than by the average molecular weight. To our knowledge, the adsorption mechanism of PAA onto mineral has always been studied with disperse polymers. Obviously, these preliminary results suggest the importance of revisiting the adsorption mechanism, now that "monodisperse" PAA is available through RAFT polymerization.

Conclusion

The preparation and use of PAA by RAFT controlled radical polymerization was presented. Using CTA **1** and **2**, the polymerization is controlled at low conversion. However, at higher conversion, and for high [AA]:[CTA], transfer to solvent occurs. This transfer becomes inconspicuous when samples are precipitated or purified before analysis by GPC. Transfer to solvent is severe in 2-propanol but also occurs in ethanol, dioxane, and methanol. Transfer to polymer occurs when polymerization is led to completion. Because of transfer reactions occurring at high conversion and high [AA]:[CTA], block copolymers having an AA first block can only be prepared if the AA segment is short.[21] Targeting longer AA blocks would result in low blockiness due to the generation of short solvent-transferred chains during the AA polymerization.

The low molecular weight polymers prepared by RAFT were used for the dispersion of kaolin, $CaCO_3$, and TiO_2. Because of the low PDI of the RAFT polymers, the dispersions are less viscous than with conventional radical polymers. These findings well agree with the predicted adsorption mechanism of PAA onto $CaCO_3$.[36] We pursue our work in this direction to now further understand the mechanism of interaction of PAA with the mineral surface.

Supporting Information Available: Kinetics of polymerizations and additional MALDI TOF spectra. This material is available free of charge via the Internet at http://pubs.acs.org.

References and Notes

(1) Buchholz, F. L. In *Ullmann's Encyclopedia of Industrial Chemistry*; Hawkins, S., Schulz, G., Eds.; VCH: Weinheim, 1992; Vol. A21, p 143.
(2) Vedula, R. R.; Spencer, H. G. *Colloids Surf.* **1991**, *58*, 99. Tjipangandjara, K. F.; Somasundaran, P. *Adv. Powder Technol.* **1992**, *3*, 119. Uchida, N.; Kabutoya, W.; Yamashita, K.; Zhang, Y.; Uematsu, K. *Key Eng. Mater.* **1999**, *161−163*, 133.
(3) Kriz, J.; Masar, B.; Plestil, J.; Tuzar, Z.; Pospisil, H.; Doskocilova, D. *Macromolecules* **1998**, *31*, 41. Kitano, T.; Fujimoto, T.; Nagasawa, M. *Polym. J.* **1977**, *9*, 153. Smid, J. *Chemtracts: Macromol. Chem.* **1991**, *2*, 399.
(4) Suau, J. M. "Coatex, Internal report", 2001.
(5) Odell, P. G.; Veregin, R. P. N.; Michalak, L. M.; Brousmiche, D.; Georges, M. K. *Macromolecules* **1995**, *28*, 8453. Puts, R. D.; Sogah, D. Y. *Macromolecules* **1996**, *29*, 3323.
(6) Patten, T. E.; Matyjaszewski, K. *Adv. Mater. (Weinheim, Ger.)* **1998**, *10*, 901.
(7) Ladaviere, C.; Doerr, N.; Claverie, J. *Macromolecules* **2001**, *34*, 5370.
(8) Mitsukami, Y.; Donovan, M. S.; Lowe, A. B.; McCormick C. L. *Macromolecules* **2001**, *34*, 2248. Sumerlin, B. S.; Donovan, M. S.; Mitsukami, Y.; Lowe, A. B.; McCormick, C. L. *Macromolecules* **2001**, *34*, 6561. Donovan, M. S.; Lowe, A. B.; Sumerlin, B. S.; McCormick, C. L. *Macromolecules* **2002**, *35*, 4123. Taton, D.; Wilczewska, A. Z.; Destarac, M. *Macromol. Rapid Commun.* **2001**, *22*, 1497.
(9) These PAA standards were made by conventional radical polymerization of AA followed by a series a precipitation/separation in selective solvents. Their molecular weight were determined by MALDI TOF and light scattering. For details on this fractionation technique, see for example: Baxendale, J. H.; Bywater, S.; Evans, M. G. *Trans. Faraday Soc.* **1946**, *42*, 675.
(10) Bessiere, J. M.; Boutevin, B.; Loubet, M. *Polym. Bull. (Berlin)* **1993**, *30*, 545.
(11) Chiefari, J.; Chong, B. Y. K.; Ercole, F.; Krstina, J.; Jeffery, J.; Le, T. P. T.; Mayadunne, R. T. A.; Meijs, G. F.; Moad, C. L.; Moad, G.; Rizzardo, E.; Thang, S. H. *Macromolecules* **1998**, *31*, 5559.
(12) Chiefari, J.; Mayadunne, R. T. A.; Moad, G.; Rizzardo, E.; Thang, S. H. In *Controlled/Living Radical Polymerization*;

Matyjaszewski, K., Ed.; ACS Symp. Ser. 768; American Chemical Society: Washington, DC, 2000; p 297.
(13) Hawthorne, D. G.; Moad, G.; Rizzardo, E.; Thang, S. H. *Macromolecules* **1999**, *32*, 5457.
(14) Charmot, D.; Corpart, P.; Adam, H.; Zard, S. Z.; Biadatti, T.; Bouhadir, G. *Macromol. Symp.* **2000**, *150*, 23.
(15) Chiefari, J.; Jeffery, J.; Mayadunne, R. T. A.; Moad, G.; Rizzardo, E.; Thang, S. H. *Macromolecules* **1999**, *32*, 7700. Mayadunne, R. T. A.; Rizzardo, E.; Chiefari, J.; Chong, B. Y. K.; Moad, G.; Thang, S. H. *Macromolecules* **1999**, *32*, 6977. Mayadunne, R. T. A.; Rizzardo, E.; Chiefari, J.; Krstina, J.; Moad, G.; Postma, A.; Thang, S. H. *Macromolecules* **2000**, *33*, 243.
(16) Bender, M. T.; Saucy, D. A. In *Column Handbook for Size Exclusion Chromatography*; Wu, C. S., Ed.; Academic Press: San Diego, 1998; p 554.
(17) In our hands, repeated methylation of the polymer, either by methyl iodide or by diazomethane, gave yields below 99% (98.4% for three treatments with MeI, 94.3% for two diazomethane treatments, as measured by residual acid titration). This precluded the accurate determination of molecular weight by organic GPC.
(18) Quiclet-Sire, B.; Zard, S. Z. *J. Am. Chem. Soc.* **1996**, *118*, 9190.
(19) Rizzardo, E.; Chiefari, J.; Chong, B. Y. K.; Ercole, F.; Krstina, J.; Jeffery, J.; Le, T. P. T.; Mayadunne, R. T. A.; Meijs, G. F.; Moad, C. L.; Moad, G.; Thang, S. H. *Macromol. Symp.* **1999**, *143*, 291.
(20) Uzulina, I.; Kanagasabapathy, S.; Claverie, J. *Macromol. Symp.* **2000**, *150*, 33. Farcet, C.; Lansalot, M.; Pirri, R.; Vairon, J. P.; Charleux, B. *Macromol. Rapid Commun.* **2000**, *21*, 921.
(21) Gaillard, N.; Guyot, A.; Claverie, J. *J. Polym. Sci., Part A: Polym. Chem.* **2003**, *41*, 684.
(22) Pichot, C.; Pellicer, R.; Grosstete, P.; Guillot, J. *J. Makromol. Chem.* **1984**, *185*, 113.
(23) Ahmad, N. M.; Heatley, F.; Lovell, P. A. *Macromolecules* **1988**, *21*, 2822.
(24) Farcet, C.; Belleney, J.; Charleux, B.; Pirri, R. *Macromolecules* **2002**, *35*, 4912.
(25) Pretsch, E.; Clerc, T.; Seibl, J.; Simon, W. *Spectral Data for Structure Determination of Organic Compounds*; Springer-Verlag: Heidelberg, Germany, 1989.
(26) Ahmad, N. M.; Lovell, P. A.; Heatley, F. *Polym. Prepr. (Am. Chem. Soc., Polym. Chem.)* **2002**, *43*, 652.
(27) In the Lovell paper, the right member constant is 0.8. The value 1.3 comes from the fact that trithiocarbonates are "difunctional"; the molecular weight of the chain during the reaction is the double of the one found in GPC.
(28) Flory, P. J. *J. Am. Chem. Soc.* **1937**, *59*, 241. Flory, P. J. *J. Am. Chem. Soc.* **1947**, *69*, 2893.
(29) Beyou, E.; Chaumont, P.; Chauvin, F.; Devaux, C.; Zydowicz, N. *Macromolecules* **1998**, *31*, 6828. Schilli, C.; Lanzendorfer, M. G.; Muller, A. H. E. *Macromolecules* **2002**, *35*, 6819.
(30) Goto, A.; Sato, K.; Tsujii, Y.; Fukuda, T.; Moad, G.; Rizzardo, E.; Thang, S. H. *Macromolecules* **2001**, *34*, 402.
(31) Tsujii, Y.; Ejaz, M.; Sato, K.; Goto, A.; Fukuda, T. *Macromolecules* **2001**, *34*, 8872.
(32) Monteiro, M. J.; de Brouwer, H. *Macromolecules* **2001**, *34*, 349.
(33) de Groot, K.; Duyvis, E. M.; Koninklijke-Shell, R. *Nature (London)* **1966**, *212*, 183.
(34) Mishra, S. K. *Int. J. Mineral. Proc.* **1978**, *5*, 69. Patil, M. R.; Shivakumar, K. S.; Prakash, S.; Rao, R. B. *J. Surf. Disp. Sci.* **1998**, *14*, 208.
(35) Rogan, K. R.; Bentham, A. C.; Beard, G. W. A.; George, I. A.; Skuse, D. R. *Trends Colloid Interface Sci.* **1994**, *97*, 97.
(36) Geffroy, C.; Persello, J.; Foissy, A.; Lixon, P.; Tournilhac, F.; Cabane, B. *Colloids Surf., A: Phys. Eng. Aspects* **2000**, *162*, 107.
(37) Bohmer, M. R.; Sofi, Y. E.; Foissy, A. *J. Colloid Interface Sci.* **1994**, *164*, 126. Dupont, L.; Foissy, A.; Mercier, R.; Mottet, B. *J. Colloid Interface Sci.* **1993**, *161*, 455. Aoudj, S.; Balard, H.; Dupont, L.; Foissy, A.; Aouak, T. *Eur. Polym. J.* **1994**, *38*, 1211.

MA0256744